A review of passive and active mixing systems in microfluidic devices

James Green[*], Arne E. Holdø[**], Aman Khan[†]
[*] Weir Strachan & Henshaw, PO Box 103, Ashton Vale Road, Bristol, BS99 7TJ, UK
E-mail: james.green@weirsandh.com
[**] Department of Aerospace, Automotive and Design Engineering, University of Hertfordshire, College Lane, Hatfield, Herts, AL10 9AB, UK.
[†] Research & Development Department, Unipath Ltd, Priory Business Park, Bedford, MK44 3UP, UK

ABSTRACT

A review of mixing elements and devices for microscale fluidic devices is presented. The application, principles and characterisation of these devices is discussed, and the classifications based on these factors highlighted. A review of published works relating both experimental and simulation profiling of both passive and active mixing systems is presented. Each mixing principle upon which a design is based is discussed with regard to the fundamental physics that governs fluid behaviour. Passive systems covered include multi-lamination, split/recombination, chaotic advection, jet based, recirculation and droplet internal convection. Active systems covered include longitudinal and transverse pulsing, micro-stirrers, electro-kinetic methods, and acoustic/ultrasonic excitation. The review shows that the majority of devices have been designed within the past five years. Furthermore, at present, devices based on the multi-laminate method appear to outperform most other systems.

1. INTRODUCTION

The subject of fluidic mixing in microscale geometry has received significant attention in recent years, with a number of authors reporting various methods of inducing and improving mixing. The high surface to volume ratio of microfluidic systems mean that they are suitable to a number of applications, including chemical synthesis (Refs. 1, 2, 3, 4, 5 & 6), DNA extraction and analysis (Refs. 7, 8 & 9), clinical diagnostics (Refs. 10, 11 & 12), and continuous analysis systems (Refs. 13, 14, 15, 16, 17 & 18). For all the applications described above, a major limiting factor of the device effectiveness is the efficiency with which mixing is achieved. Multiple mixing systems are sometimes used within the same device, and many methods promote mixing by being based on more than one principle.

Apart from the variety of applications of microfluidic devices mentioned above, the reason that microfluidic mixing has received such interest is that it is at present relatively difficult to achieve quick and efficient mixing when the characteristic length scale of the system is small (Ref. 19). In macroscale mixers, such as industrial stirrers and gas turbine combustion chambers, turbulent eddies provide a quick and efficient method of mixing. The

classical method of quantifying the turbulent nature of a fluid flow is through examination of the Reynolds number, defined as;

$$\mathrm{Re} = \frac{\rho \cdot u \cdot d}{\mu} \tag{1}$$

Where ρ is the density, u is the fluid velocity, d is a length scale that characterises the system, and μ is the absolute viscosity.

It is commonly accepted that in steady pipe flow, the transition from laminar to turbulent flow occurs in the region of Re = 2300. For the case of water (ρ = 1000 kg.m^{-3}, μ = 0.001 kg.m^{-1}.s^{-1}) travelling at 1 m.s^{-1} in a 1000 mm channel, the resultant Reynolds number is Re = 1000, which indicates the flow is within the laminar regime. As can be seen from the form of eqn (1), reducing the characteristic length scale of the system will produce a proportional reduction in the Reynolds number. As such for similar flow conditions in a 10 μm channel, the resulting Reynolds number would be Re = 10.

Consequently, in microscale geometries, turbulence is generally absent, and as such the mixing is limited to diffusion, and any additional mixing must be artificially induced. Figure 1 shows an example of the lack of mixing that can occur in a microfluidic geometry.

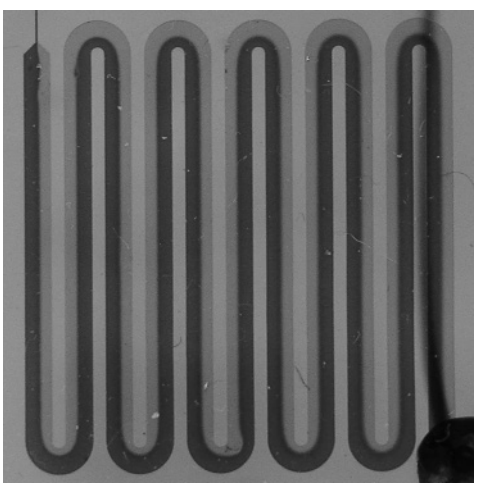

Figure 1 Photograph of the laminar flow of yellow and blue food dye in a 1 mm width, 100 μm depth and centreline length of 190 mm serpentine channel with a volumetric flow rate of roughly 5×10^{-9} m^3.s^{-1}. Note the lack of efficient mixing and the negligible increase in diffusion layer size [source: 20].

Here the flow has a Reynolds number of 50 based on channel width, and as such is completely laminar. The diffusion layer between the two fluid streams barely increases along the channel length, and the two streams are still fully distinct as they exit the chip. Hence it can be seen why it is necessary to improve mixing in low Reynolds number flows.

Another important dimensionless group used for characterising a system is the Schmidt number, given by

$$\mathrm{Sc} = \frac{\upsilon}{D} \tag{2}$$

where υ is the kinematic viscosity and D is the diffusion coefficient, and relates the ratio of viscous to diffusive transport. For gaseous mixing, the Schmidt number is typically Sc ≈ 1, and therefore diffusion and viscous action are comparable. However, in liquids, the Schmidt number is typically Sc ≈ 600 – 3000, and therefore viscous action dominates over diffusion, meaning that fluid convection is more important than diffusion to the mixing process (Ref. 21).

The governing equations of fluid mechanics are based around the conservation principles of mass, momentum and energy. For the purposes of discussing the mixing in microfluidic devices, the equations that model the preservation of momentum for a viscous fluid – known as the Navier-Stokes equations – are examined, and for a Newtonian fluid are given as

$$\rho \frac{D\mathbf{U}}{Dt} = \rho\mathbf{a} - \nabla p + \mu\nabla^2\mathbf{U} \tag{3}$$

where ρ is the bulk density, **U** is the velocity vector, **a** is the acceleration due to a body force (e.g. field affects such as gravity, magnetism etc), p is pressure and μ is the absolute viscosity. The body force and pressure gradient terms can be classified as source terms, since they represent sources of momentum. The LHS of eqn (3) represents the resultant motion of a fluid as a result of the sources of momentum and the internal shearing stress (the viscosity term). Therefore, fluid motion can be produced by inducing a pressure gradient, by shearing the flow (as used in stirrers), by using an external field effect, or any combination of the above.

2. BASICS OF MIXING

In order to appreciate the literature that has been published in relation to micro mixer devices, the basic principles underlying mixing must be studied. In laminar flows, any mixing that occurs is limited by the diffusivity of the two phases, and as such it is important that diffusivity be examined more closely. The conservation of a chemical species can be expressed as;

$$\frac{\partial}{\partial t}\left(\rho w_i\right) + \nabla \bullet \left(\rho \mathbf{U} w_i\right) = \nabla \bullet \left(D_i \nabla\, w_i\right) + S \tag{4}$$

where w_i is the mass fraction of species i and S represents additional sources such as body forces, boundary conditions, chemical reactions etc. (Ref. 22). The diffusive flux term on the RHS of eqn (4) is derived from Fick's 1st law, where a flux is defined as the rate of fluid flow through a given area. As such the rate of diffusive mass transfer can be rearranged to give;

$$\frac{1}{t_D} = D_i \cdot A \cdot \nabla w_i \tag{5}$$

where A is the diffusion area.

From these two equations the factors that can be altered to increase the rate of mixing in a microfluidic device can be examined. From eqn (5) it can be seen that the mixing rate is proportional to the diffusion coefficient, the area across which diffusion can occur, and the

concentration gradient, therefore increasing these factors will lead to an increase in diffusive mixing. Modification of the diffusion coefficient is not always an option depending on the nature of the substances being mixed. For the case of mixing particulates with a suspending fluid, then it is possible that some modification to the diffusion coefficient can be achieved. If the particles can be considered as Brownian, then an increase in temperature and reduction in particle radius would lead to an increase in the Brownian diffusion coefficient, as described by;

$$D_B = \frac{k \cdot T}{6\pi \cdot \mu \cdot a} \tag{6}$$

where k is the Boltzmann constant, T is the temperature, and a is the particle radius (Ref. 23). If irreversible hydrodynamic interactions leading to a shear induced diffusion type process are present, then the diffusion coefficient is typically

$$D_\tau \propto \dot{\gamma} \cdot a^2 \cdot \phi^2 \tag{7}$$

where $\dot{\gamma}$ is the strain rate, and ϕ is the particle volume fraction (Refs. 24, 25 & 26). As can be seen, in this case an increase in particle size and strain rate will result in larger diffusive fluxes.

Besides modification of the diffusion coefficient, the other options are to increase the area over which diffusion can occur, and to increase the concentration gradient. Both of these methods are utilised in current devices, often with one being the side effect of trying to increase the other (see below).

As the mixing process progresses, it is natural for the concentration gradient to flatten, and therefore we would expect to see a reduction in the mixing with time.

With regard to the form of eqn (4), and the implications for mixing, it can be seen that the inertial and diffusive fluxes are in direct proportion to one another, and therefore if it is wished to increase the diffusive fluxes, the inertial fluxes must be increased (assuming that sources of concentration remain the same). The inertia terms of eqn (4) are split into the temporal and convective acceleration terms, which equate to changes in speed and direction respectively. Therefore, it can be said that rapid changes in speed and/or direction will lead to an increase in the diffusive fluxes. Rapid pulsing of the flow has been reported by various authors as an effective method of mixing (Refs. 27, 28 & 29). Other authors have harnessed convective acceleration by forcing the fluid to follow a particularly tortuous route (Refs. 30, 31 & 32), which also shows an increase in mixing.

2.1 QUANTIFICATION OF MIXING

When discussing mixing, it is useful to state the dimensionless groups often used to characterise the mixing process. The Peclet number is the ratio of convective to diffusive fluxes, and is given by

$$\mathrm{Pe} = \frac{u \cdot d}{D} \tag{8}$$

The Fourier number is defined as

$$\mathrm{Fo} = \frac{t_r}{t_D} \tag{9}$$

where t_r is the residence time, given by

$$t_r = \frac{L}{u} \tag{10}$$

where L is the channel length under consideration. The mixing time t_Γ is given by

$$t_\Gamma = \frac{d^2}{D} \tag{11}$$

The Peclet number can be used in a variety of ways. For processes with a constant coefficient of diffusivity, the Peclet number is directly proportional to the flow rate through the device.

The Fourier number is simply the ratio of residence time to mixing time, so a Fourier number less than one indicates that the residence time is sufficient for mixing to occur. A Fourier number greater than one indicates that complete mixing is not achievable for the given geometry and flow rate, and may be reduced by either increasing the length of the channel, reducing the flow rate, or decreasing the characteristic length scale.

Methods of experimentally measuring concentration distribution and mixing vary, but many are either visual or imaging based. Fluorescence intensity is widely used (Refs. 33, 34 & 35) although this suffers from the usual problems of attenuation and background noise. Time averaged methods such as Time Resolved Fluorescence (TRF) or Luminescent Oxygen Channelling Immunoassay (LOCI) type methods are less common (Refs. 36, 37 & 38). Another problem affecting fluorescence methods is that a substance either fluoresces or it does not, meaning that concentration gradients are difficult to visualise and quantify using this method.

Dye methods have been reported as offering greater visualisation of concentration gradients than fluorescence methods (Ref. 39). Image processing tools can then be used to derive quantitative data regarding concentration profiles throughout the channel under consideration.

Visualisation methods based on pH are also reported in a number of devices (Ref. 40). These changes in colour are generally the result of chemical reactions, and as such can be very application specific, with the advantages and disadvantages that come with that.

Methods for actually evaluating the extent and quality of the mixing achieved within a device are commonly statistical in nature. Homogeneity is defined as the ‘uniformity of composition’ of a mixture. As such, a common statistical method for determining and quantifying variations within a data set is the standard deviation, which is simply the sum of the variances divided by the number of data points. A variant of this method was utilised in Ref. 41, where the coefficient of mixing was defined as:

$$C_{\mathrm{mix}} = \frac{C_{\mathrm{dev\,in}} - C_{\mathrm{dev\,out}}}{C_{\mathrm{dev\,in}}} \tag{12}$$

Where C_{dev} is calculated at the inlet and outlet, and is given by

$$C_{\text{dev}} = \frac{\sqrt{\frac{1}{N}\sum_{i=1}^{N}\left(I_i - \bar{I}\right)^2}}{2^n - 1} \tag{13}$$

where I is the fluorescent intensity. Examining eqn (13) reveals that the numerator is the standard deviation of the intensity distribution, normalised by the gray level amplitudes, where n is the gray bit number of the image (denominator) i.e. normalising for the overall brightness from one image to the next. Using this method leads to a C_{mix} value of 1 for a completely homogeneous solution, and a value of 0 for a when no mixing occurs within a given channel.

The work reported in Ref. 42 derived a mixing percentage (ϕ) from CFD data using the following formula.

$$\phi = \left(1 - \frac{\sum_{i=1}^{n}\left|\left(N_i - \bar{N}\right)V_i\right|}{\sum_{i=1}^{n}\left|\left(N_i - \bar{N}\right)V_i\right|_o}\right) \times 100\% \tag{14}$$

where N_i is the mole fraction in question and V_i is the local cell volume. Note that if the specifics relating to normalisation and data correction are ignored, both eqns (13) and (14) calculate standard deviation.

This statistical data can be derived from a number of sources. Results can be calculated from CFD simulations by using every cell as a sample point, or a block/slab of cells as required, and then the data output. This is especially useful since in the case of a transient simulation, it is possible to look at how the mixing progresses with time. For experimental studies using dyes or pH indicators, image processing on a pixel-by-pixel basis can also produce useful data on mixture homogeneity.

3. MIXING CLASSIFICATION

It is possible to classify the various reported mixing devices by the manner in which they encourage mixing, and the type of fluid flow for which they are intended. One classification that has been present in the literature for some time is the distinction between passive and active mixing systems. Passive systems could be defined as a system requiring no external power source to function, although this classification would then only incorporate surface tension and gravity driven flows, since you could argue that pumps, electric fields etc require an external power source. Instead, passive systems are defined as mixing systems that mix through virtue of their geometry and any natural flow features that arise. Active systems are defined as methods that force the fluid to behave in a manner that cannot be achieved through geometry alone. Therefore the use of pumps and electric fields for reasons of mixing rather than simple locomotion would be classified as an active mixing system.

Passive systems are generally more desirable since they are generally more reliable (due to a reduction in the number of moving parts), and since they require no extra power source, they do not put any extra strain on the total system power supply. One of the key attractions of microdevices is their portability and low power requirements, and as passive mixing systems require no extra power, they conform well to the design philosophy above.

If power supply is not an issue, or if superior mixing speeds are required by a device's application, then active mixing systems may be adopted. These tend to work in a variety of different and novel ways, and if well designed, can offer superior mixing times to many passive methods.

Another method of classifying a mixing process is defined in Ref. 21, and relates the significance of the mixing process to overall flow dynamics. Level 1 or non-coupled mixing is defined as where the mixing process has no overall effect on the flow dynamics. Examples are density matched fluids and low concentration mixing, where the mixing process does not produce significant gradients in the physical properties such as density and viscosity. Scalars such as ink dyes and tracer particles can generally be categorised as non-coupled.

Level 2 or coupled mixing is defined as where the mixing process is coupled with the flow dynamics through significant variations of the physical properties by a variation in concentration, so that density and viscosity vary significantly with the degree of mixing. Examples include the mixing of bi-density fluids or suspensions in the presence of gravity, or anisothermic gaseous mixing where buoyancy is significant. In all these cases, the mixing process must be correctly modelled to fully describe the flow dynamics.

Level 3 or source-coupled mixing is defined as where the mixing process produces sharp changes in the fluid properties, significant enthalpy conversion or high pressure changes. This classification incorporates highly endo/exothermic reactions such as combustion, detonation and nuclear processes, where reaction products manifest as sources of concentration, heat and momentum. These sources often dominate the flowfield, and therefore are strongly coupled back onto the mixing process.

4. PASSIVE MIXING METHODS

In this section, the current practices used to perform passive mixing in microfluidic devices shall be discussed. Each subsection ends with a table summarising important features and references.

4.1 MULTI-LAMINATION METHODS

Many passive mixing systems used multi-lamination techniques to increase the area across which diffusion can occur. Multi-lamination generally involves bringing multiple fluid streams together in one channel, creating alternating layers of differing fluids, thereby substantially increasing the diffusion area when compared to a two stream system. If we consider the example given in Figure 1, where the channel depth is 100 μm and the length is 190 mm, then the diffusion area is $A = 1.89\times10^{-5}$ m^2. If the number of streams were to be increased from two to four, the diffusion area would increase to 300% of the original. This can be seen from eqn (5), which shows that an increase in diffusion area leads to an increase in diffusion rate.

When considering multi-lamination methods, there are really two important factors, the diffusion or intermaterial area, and the striation thickness. The striation thickness can be related to the diffusion area per unit volume by the following equation (Refs. 43 & 44).

$$s \approx \frac{1}{a_v} \tag{15}$$

Therefore, by measuring or predicting the average gap between striations/laminae, we can calculate the diffusion area per unit volume, and as such we can examine the efficiency of a device with regard to increase in diffusion area.

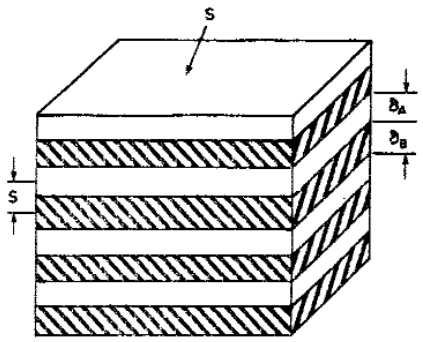

Figure 2 Idealised multi-laminate striations, showing the definition of the striation gap [source: 43].

One reported device (Ref. 45) combines two fluid streams into a 16 stream channel, and achieves 95% mixing, based on fluorescence intensity, within 15 ms, and complete homogeneity is achieved in less than a second. Reynolds numbers varied between $0.5 < Re < 31$, but since no data on diffusivity is presented, the system cannot be characterised by Peclet and Fourier numbers. In this device, the configuration resulted in 30 striations across the channel following the mixing section, which for a channel width of 150 μm, results in an average striation gap of 5 μm.

Another reported device (Ref. 39 & 46), utilises a striation gap of 85 μm, and good mixing is achieved within 2.4 mm of the stream combination, at a Reynolds number of Re = 0.03. Dye visualisation methods were used in the reported experiments, and concentration gradient data was obtained using image processing techniques.

The device reported in Ref. 47 uses a lamination technique to encapsulate bovine serum albumin (BSA) in a polymeric coating. Dispersed BSA and polymer dispersion is mixed with an extraction fluid into multiple laminae, which rapidly breakdown into droplets which formed the required microspheres. This technique is of use in the pharmaceutical industry, for the production of therapeutic drugs.

The work reported in Ref. 48 examined the use of multilamination type mixers to create foams, by mixing gas and liquids together. The study was intended as a basic examination of the effect of mixer geometry on bubble size, using standard off the shelf mixers, primarily intended for liquid/liquid mixing. As expected, non-uniform bubble sizes resulted, highlighting the application specific nature of many micromixers. Smaller feed-in channel geometries resulted in the smallest bubble sizes, and certain mixer geometries resulted in higher bubble size distributions than others. This work is of interest since it is the first example to be presented here of level 3 mixing. By interspersing a gaseous phase within a liquid phase, we introduce density discontinuities and surface tension effects, leading to strong local pressure gradients.

Table 1 Multi-lamination summary.

Mixing mechanism	Increase in diffusion area
CFD models	Diffusive scalars
Flow visualisation	Dye, fluorescence, acid/base indicator
Mixer size	Typically 10 x 10 mm
References	43-48

4.2 Y/T/X JUNCTION CHANNELS

The use of a Y/T/X junction channel to combine two or more separate flows that are to be mixed is a common feature of many mixing devices (Refs. 49, 50 & 51). Assuming a basic laminar flow pattern without extra mixing geometry, following the junction there is a single area across which diffusion can occur, therefore the mixing event at the junction is of outmost importance to the mixing performance of the device. Many devices utilise high flow rates to increase Reynolds numbers to transition or fully turbulent values, which significantly improves the mixing rate. Researchers in this field typically characterise the flow in the junction according to three flow regimes:

[i] Stratified – where the flow is characterised by smooth streamlines that follow the channel geometry. Mixing is diffusion limited and therefore reduces with Reynolds number due to the reduction in residence time.

[ii] Vortex – where vortices begin to build up within the channel. Here the reduction in residence time is balanced by the increase in diffusion area brought about by the vortices "stretching" the flow.

[iii] Engulfment – where axial symmetry is lost and streamline entwining leads to a significant improvement to mixing with increasing Reynolds number.

This three regime behaviour is generally only seen in micron scale junction devices, since larger scale are generally run at more turbulent flow regimes (Ref. 52).

An early example of a junction type micromixer is given in Ref. 40, where a T junction was used to hydrolyse phenyl chloroacetate (PCA). Results showed that the hydrolysis reaction completed within 110 μs when complete mixing was achieved. The range of volumetric flow rates examined was $0.2 < Q < 2.5$ mL/s, which for the device under consideration equates to a Reynolds number range of $400 < \mathrm{Re} < 4400$. From this the transition from laminar to turbulent flow should occur at $Q \approx 1.3$ mL/s. The authors of Ref. 40 noted that flow rates of $Q > 0.5$ mL/s are sufficiently turbulent to achieve very efficient mixing.

Figure 3 from Ref. 53 shows dye visualisation of flow patterns in a T junction mixer at various inlet pressures, and illustrates the three aforementioned flow regimes. As can be seen, at the $\mathrm{Re} \approx 211$ condition, the flow is laminar with very little mixing occurring. At $\mathrm{Re} \approx 388$, the flow patterns are unsteady, with a significant amount of interweaving due to the onset of vortex formation. At $\mathrm{Re} \approx 588$, the two liquids mix rapidly at the T junction due to the onset of turbulent fluctuations, which as mentioned above is commonly termed the engulfment regime. All the designs examined in this study tend to produce rapid mixing when $\mathrm{Re} < 440$.

The work reported in Ref. 54 examines both T and Y junction geometries using CFD. The work examined gaseous mixing, namely methanol and oxygen. Reynolds numbers in gaseous flows are typically lower than in liquid flows, since the density to viscosity ratio is much lower. For water, $\rho/\mu = 1\times10^6$, whereas for air at STP, $\rho/\mu = 6.6\times10^4$, meaning that for similar velocities in the same geometry, the Reynolds number of a gaseous flow will be about two orders of magnitude smaller than liquid flow. For the work mentioned above, the typical gaseous Reynolds number was $\mathrm{Re} \approx 6$, and hence the flows were very laminar. Since the mixing in this case is diffusion dominated, reductions in inlet velocity lead to reductions in the mixing length, since it allows for a greater residence time. This is the reverse of the work from Ref. 53, where the mixing was turbulence dominated, and as such increased in-flow velocity lead to greater turbulent fluctuations. Knudsen numbers in Ref. 54 typically varied between $10^{-3} < \mathrm{Kn} < 10^{-1}$, a range where wall slip conditions become significant, and were accounted for in the simulations.

Additional surface structures in the vicinity of the junction mixer can have a significant impact on mixer, as demonstrated in Ref. 55. In this example, wells slanted at 45° to the bulk flow direction placed subsequent to the T junction significantly improved the length required to complete mixing. 80% mixing was achieved within 440 μm of the junction with the structures, whereas without the structures 80% mixing required 2.3 cm, an improvement of 98%. The channels examined in Ref. 56 were X junction based, with cuboid static mixing structures on the channel walls. With Reynolds numbers up to 300, and flow obstructions extending 33% of the channel width into the flow, mixing was achieved in the near lee region of the structures, and within 0.5 ms of pressure being applied to the system. Areas of recirculation were present in lee of the cuboid structures, and the large transverse velocity component made a significant improvement to the mixing efficiency.

Table 2 Junction summary

Mixing mechanism	Increase in diffusion area Onset of turbulence
CFD models	Diffusive scalars Particle tracking Turbulence
Validation examples	49, 50, 52, 54
Flow visualisation	Dye, acid/base indicator, fluorescence
Mixer size	Typically 6 x 6 mm.
References	49-56

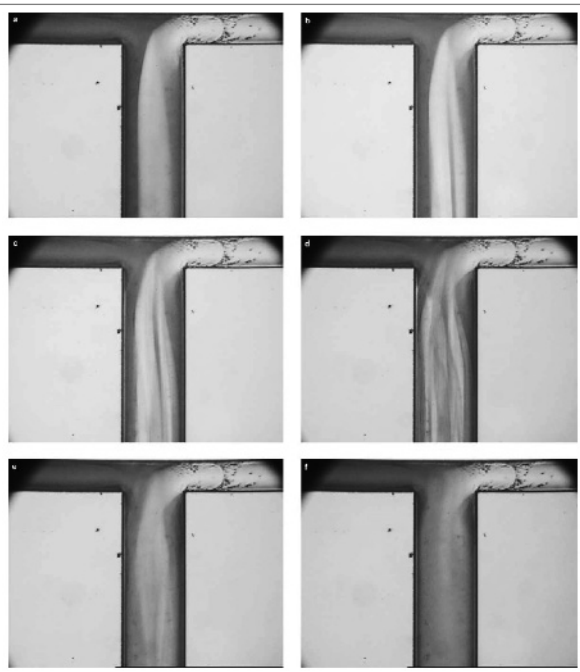

Figure 3 Dye visualisation of the flow patterns and mixing in a T junction at various inlet conditions, listed respectively from picture (a) to (f) as, Re ≈ 211, 313, 342, 388, 423 and 588 [source: 53].

4.3 SPLIT/RECOMBINATION METHODS

Another method based on the multi lamination principle is that of split/recombination methods, where a heterogeneous mixture is split and recombined in such as way as to increase the diffusion area.

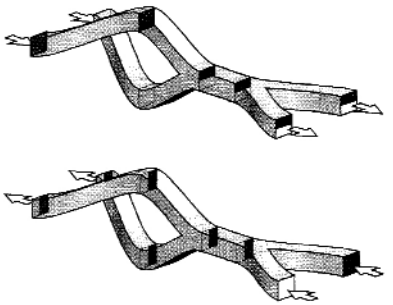

Figure 4 Generic split/recombination type mixer geometry [source: 57].

The geometry outlined in Figure 4 shows the basic principle of split/recombine methods. Two streams are initially combined with a horizontally aligned diffusion area, which is then split again, and would be recombined in a manner that produces multiple laminates. This method can also be applied to splitting the flows into horizontal laminates, which can then be stacked along the flow direction to produce multiple diffusion areas with multiple alignments. This stacking is often referred to in the literature as successive split-and-recombine (SAR) methods.

One paper that fully examines the mixing efficiency and flow features of a SAR device was Ref. 58, where CFD simulation results were validated against experimental data. Figure 5 shows a visualisation of the multi-lamination induced by the mixer geometry.

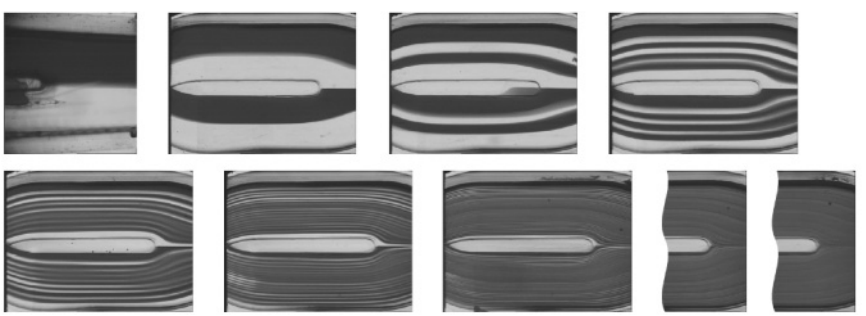

Figure 5 Multi-lamination of dyed and pure water in a SAR type micromixer, shown at Re = 0.22 [source: 58].

As can be seen, each stage of the split/recombine geometry doubles the number of lamina, effectively doubling the diffusion area. By the eighth stage, the distance between strata has become very small compared to the channel width, and an almost completely homogenised mixture is achieved. For the work described above, the length of each step in the SAR mixer was 6mm, meaning that the mixture illustrated in Figure 5 would require a mixer of length 48mm, which is obviously very compact.

This paper also illustrated the appearance of chaotic advection at higher Reynolds numbers (Re < 15 approx.). Whereas some devices utilise chaotic advection to improve the mixing process (see below), in this device, the higher Reynolds numbers (Re < 30) resulted in separation of the fluid from the channel at the point of recombination. This reduced the multi-lamination effect, thereby reducing the mixing. This problem could be alleviated by scaling up the size of the micro mixer, although excessive scaling should be avoided to ensure diffusion length scales do not become small when compared with striation distances.

Another device reported in Ref. 59, compares a SAR mixer with a helical type mixer, which mixers by tortuosity and chaotic advection. The helical mixer displayed a smaller pressure drop than the SAR mixer, although simulation data suggests that the SAR mixer produces greater mixing per unit length of the device than the helical mixer.

Table 3 Split/Recombine summary

Mixing mechanism	Increase in diffusion area
CFD models	Diffusive scalars
Validation examples	56, 57, 60
Flow visualisation	Dye, fluorescence
Mixer size	Various
References	57-60

4.4 TORTUOUS CHANNELS

By forcing the fluid through a tortuous channel, the flow direction is constantly altered, leading to an increase in the convective accelerations on the LHS of eqns (3 & 4). Tortuous routes also have the effect of inducing chaotic motions in the fluid, which act to stretch and distort concentration profiles, thereby increasing the diffusion area, increasing the diffusion rate as per eqn (5). Two and three dimensional serpentine and square wave channels have been reported as an effective method of inducing the behaviour described above.

Another example of work that uses channel tortuosity to promote mixing is presented in Ref. 61. The device consists of four flow levels, constructed from nine Mylar laminates. Figure 6 illustrates the mixing effect of the channel tortuosity on the fluid streams within the device. The fluid is forced through sharp 90° turns in close succession, increasing the diffusive fluxes as per eqn (4). This process results in rapid mixing of the fluid streams. Figure 7 illustrates the overall device layout and the geometry of local structures. The two dyes are diluted within the early stages of the device (A to E), and are then combined to varying degrees, allowing for multiple mixtures of varying proportions at the outlet of the device (F).

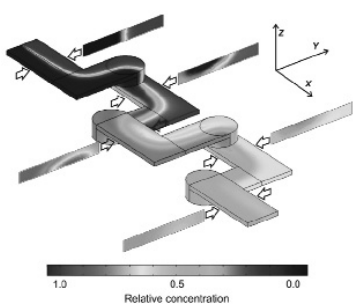

Figure 6 Mixing in a multi-layered tortuous channel [source: 61].

Table 4 Tortuous channel summary.

Mixing mechanism	Convective fluxes
CFD models	Diffusive scalars Particle tracking
Validation examples	31, 32, 35, 62, 63
Flow visualisation	Dye, fluorescence
Device size	Various
References	31-32, 35, 61-63

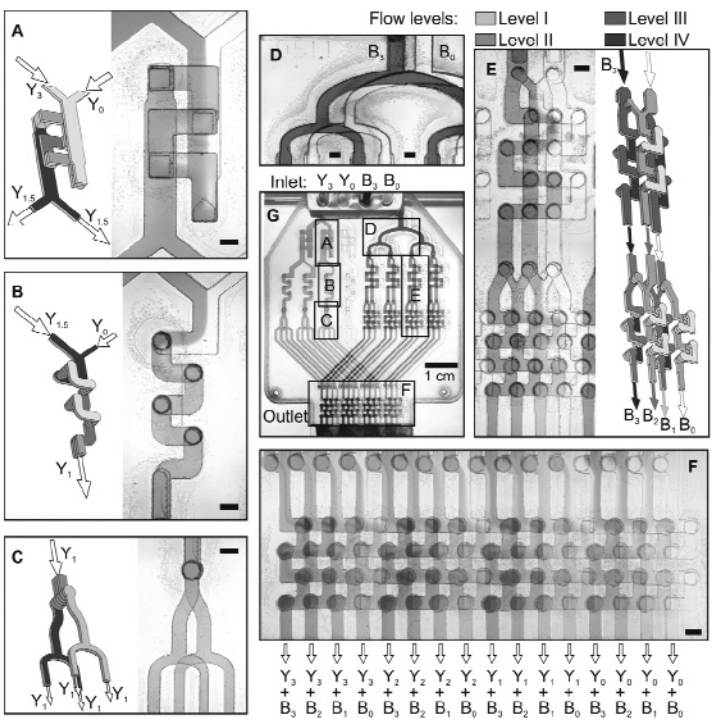

Figure 7 Use of tortuosity (A, B) to achieve mixing [source: 61].

4.5 CHEVRON SURFACE STRUCTURES

Having chevron pattern or 'herring bone' surface structures is another popular way of inducing chaotic behaviour in an adjacent fluid. This chaotic fluid motion acts to stretch and contort the concentration profile so that the diffusion area is increased, increasing the diffusion rate. The papers from Refs. 33 & 64 give excellent coverage of this process. The chevron structures reported here have a depth that is 23% of the main channel depth, and produce significant distortion of the concentration profile. Figures 8 and 9 show the affect of the surface structures on the bulk flow passing it.

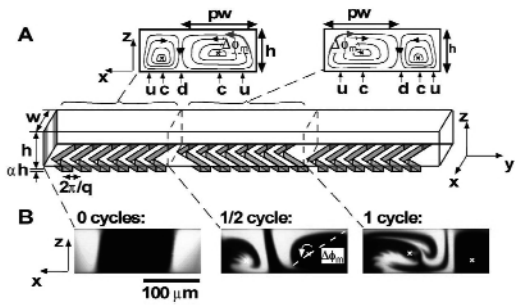

Figure 8 Diagram of chevron surface structures with predicted recirculation pattern (A) and experimental results (B). For this example, h=77 μm, w=200 μm, α=0.23, q=2π/100 μm^{-1} with 10 ridges per half cycle. [source: 33].

The distortion of the bulk flow is clear from Figure 8, and represents just the result of a single cycle of structures. Figure 9 shows the effect on the flowfield of a five cycle channel.

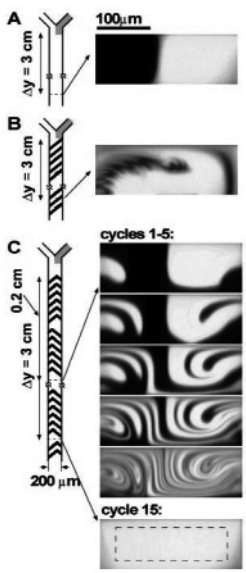

Figure 9 Affect of multiple chevron cycles on the concentration profile. Note that multiple cycles has a multi-lamination type effect. [source: 33].

The multiple cycles produce multiple laminates, significantly increasing the diffusion area. The results above were used to validate the CFD simulation work reported in Ref. 65, where a particle tracking method was used to represent the two phases. The method reported produced results that agreed exceptionally well with the experimental data from Ref. 33.

Table 5 Chevron surface structure summary.

Mixing mechanism	Increase in diffusion area
CFD models	Diffusive scalars Particle tracking
Validation examples	65, 66
Flow visualisation	Fluorescence
Mixer size	Typically 0.25 x 15 mm
References	33, 64-67

4.6 FLOW FOCUSING CHANNELS

Flow focusing can be described as a constriction of the flow, bringing multiple streams into close proximity with each other. This is equivalent to increasing the concentration gradient ∇w_i by reducing the length across which it acts, thereby increasing the diffusion rate as per eqn (5).

The work previously mentioned in the T-junction section (Ref. 53) also examined the effect of using a throttle constriction to focus the flows. It was found that the smaller the constriction, the faster the time to complete mixing, although at the expense of a high pressure drop along the throttle.

The work reported in Ref. 68 reduced two streams of 300 μm each into a single channel of 100 μm. The results showed that a low flow rate of the order of 2 μL/min was required to achieve complete mixing in the channel. This reduction in flow rate was required to increase the residence time, giving diffusion enough time to mix the two fluid streams (eqns. 7, 8 and 9). A significant pressure drop was also predicted for this channel constriction.

The work of Ref. 69 combined flow focusing with a multi-laminate flow, thereby concentrating multiple laminae within a single channel of varying dimensions. The analytical methods employed in this paper produced solutions that were computed within a minute, and could easily be adapted for other focusing or multi-laminate devices, and as such would be a useful tool in optimisation studies.

Table 6 Flow focusing summary.

Mixing mechanism	Increase in concentration gradient.
CFD models	Diffusive scalars
Device size	Various
References	53, 68-69

4.7 DROPLET BASED MIXERS

A number of researchers have recently reported the use of the natural internal motions of a droplet as an effective mixer for sub-microlitre sample volumes. The rolling motion inherent to free surface flows (Refs. 70, 71 & 72) such as droplets produce internal convection currents that act to stir the contents of the droplet (Ref. 73). By convecting the fluid, the diffusive fluxes are naturally increased as per eqn (4), and as the rolling motion tends to stretch and distort a concentration profile, the diffusion area is also increased. Once this has been realised, it is simply a case of providing impetus to the droplet, and examining the effects this driving force will have on the mixing process.

The first reported use of a liquid droplet as a mixing chamber (Ref. 9) used air pressure

to force a liquid bolus through a straight channel as part of a DNA analysis device. Unfortunately, the authors offer no discussion of how the mixing is achieved and state simply that "the drops mix together".

Another device that uses air pressure to provide impetus to the droplet (Ref. 74) goes into greater detail as to the internal droplet motions and their effect on the mixing. For a 1.25 nL droplet, mixing time was reduced from 180 s to 30 s, a six times improvement, by shuttling three times along a channel of length 1.5 mm. Figure 10 shows the improvement in mixing produced by the shuttling process.

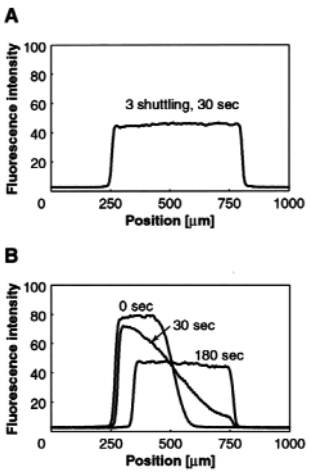

Figure 10 Plots of fluorescence intensity against longitudinal position for a shuttled (A) and diffusion limited (B) droplet showing the improvement in homogenisation produced by droplet motion. [source: 74]

It should be noted that the shuttling process as described here involves traversing the droplet back and forth within a single channel. Assuming that during the shuttling process there is no settling time at either end of the channel, then the Reynolds number based on channel depth is $Re = 7.5\times10^{-3}$. This value for Reynolds number is very close to the range for which the creeping flow approximation becomes valid, and as such flow reversibility will start to become evident. The back and forth shuttling process may have suffered from this reversibility, essentially undoing some of the mixing it had achieved every half cycle. A more ideal solution would have been for the shuttling to have been in one continuous direction, thereby not inducing any reversibility effects. The authors do concede however that this does seem to be the first reported example of experimentally proven droplet mixing.

Aside from using air pressure as the driving force, other authors have reported the use of electrokinetic wetting as a way of providing impetus to the droplet. Researchers at Duke University are developing electrowetting based droplet mixers for lab-on-a-chip style devices for clinical diagnostics.

Electrowetting is the name given to the dependence of the interfacial tension of a meniscus on the charge density accumulated at the interface (Refs. 75, 76 & 77). Devices using varying arrays of electrodes have been reported (Refs. 72 & 73), with various configurations described. The first paper (Ref. 78) describes shuttling the droplet back and forth along a linear array of electrodes. The range of Reynolds numbers examined was

$0.45 < Re < 7.2$. The flow reversibility effects described earlier are not apparent for all experiments reported here, although for the experiments involving μL scale droplets is still evident (see Figure 11). The fastest mixing time was for a linear 4 electrode array running at 16 Hz, and produced complete mixing in a 1.3 μL droplet in 4.6 s.

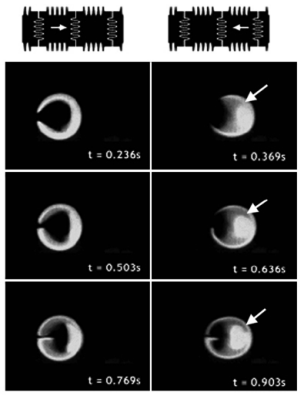

Figure 11 Reversible droplets Re ≈ 5 [source: 78]

The second paper (Ref. 79) describes non-linear array configurations that manipulate the droplet in such a way that the flow irreversibility could not become an issue. A 2×4 array operating at 16 Hz proved the best configuration reported; the complete mixing time reported using this configuration was less than 3 seconds for a 1.4 μL droplet.

With regards to analysis of the internal rolling motion of the droplet, and the subsequent effect on the mixing, a number of papers have been produced. One paper reports work examining the motion of a circular droplet (Ref. 73), as appropriate to the electrowetting examples above.

Another paper (Ref. 80), examines a droplet in a slit-type channel. The paper examines the distance between striations produced as the droplet rolls through the channel. One assumption that is made in the analysis is that the length is very large compared to the width of the channel, and that no surface tension effects are present. These assumptions lead the authors to adopt a Hagen-Poiseuille approximation for the axial velocity, which for a low aspect ratio droplet would be an inapplicable assumption, due to the significant transverse convection in the vicinity of the menisci.

It should be noted that no papers concerning CFD simulations of droplet mixers were found during the research for this article. This scarcity is probably due to the computational expense of modelling flows with surface tension effects, especially when dynamic contact angles need to be considered.

Table 7 Droplet summary.

Mixing mechanism	Increase in diffusion area.
Flow visualisation	Fluorescence
Mixer size	Various
References	9, 70-80

4.8 JET BASED METHODS

Jets are commonly used as a mixing mechanism in large scale chemical reaction processes (Refs. 81 & 82), due to their entrainment and turbulent nature. The use of micro-scale jets to mix relies not on turbulence but on an increase in diffusion area in much the same way as multi-lamination mixers. The device reported in Ref. 83 injects reagent into a sample fluid flow through an array of 400 micro nozzles, arranged with the exit plane parallel to the axial centreline of the bulk flow, so that multiple laminar jets-in-crossflow are produced. The setup described produced complete mixing in 1.2 s.

The jet based mixer reported in Ref. 84 is fairly unique in that turbulence is achieved within a micro-scale geometry. Two liquid jets emanate from rectangular exits placed one above the other, with the axial directions of the jets placed at 90° to each other, increasing the shear acting on the jets. The initially laminar flows quickly become turbulent as it emanates from the exit planes into the mixing chamber, producing rapid mixing through turbulent action. It is the additional shearing brought about by the obliqueness of the jets that result in the transition to turbulence.

Another turbulent mixer, with Reynolds numbers in the region of Re = 4000, is reported in Ref. 85. Figure 12 outlines the basic geometry of the device, with two streams of fluid A and B colliding at the junction of the four channels where turbulent mixing occurs.

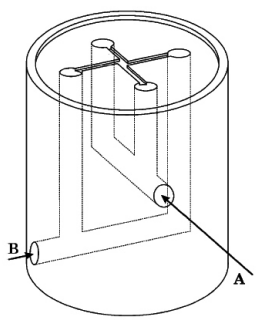

Figure 12 Schematic of the tangential micromixer, used to mix fluids A and B, where high velocities result in Reynolds numbers of 4000 at the mixer centre [source: 85].

From the diagram it can be seen that if turbulence can be generated, then simple geometries can replace the complex geometries described for other methods.

Table 8 Jet summary.

Mixing mechanism	Increase in diffusion area Onset of turbulence
CFD models	Diffusive scalars Turbulence
Validation examples	84
Device size	Various
References	81-85

4.9 NOVEL & MULTI-PRINCIPLE DESIGNS

A number of novel designs have been reported that utilise various methods to encourage mixing. One such reported example takes advantage of the Coanda effect to increase entrainment as part of a split/recombination scheme (Ref. 86). Due to the nature of the structure, an increase in flow rate achieved much better mixing results, which is slightly counter intuitive since a reduction in residence is usually associated with a reduction in the mixing. This shows that the Coanda surfaces do have a significant impact on the mixing efficiency.

Another novel design was reported in Ref. 87, where hydrophobic/hydrophilic patterned substrates were used to mix two immiscible fluids. Patches of surface treatment, attractive to just one of the two phases, were patterned in a "chess board" fashion across a wall of the microchannel, causing transverse convection, leading to intermixing.

The work reported in Ref. 42 examines the early stages of the design of a recirculation chamber, where the inlet and outlet are placed at a tangent and on opposite sides to a circular or annular chamber, with the recirculation acting to stir the flow. CFD and fluorescent particle experimental methods were used to examine the flow in the chamber, with a Reynolds number range of $10 < Re < 400$. The annular device showed recirculation near the inlet, but bulk recirculation did not occur until $Re > 150$. The circular device behaved in much the same manner, with bulk recirculation not occurring until $Re > 150$. The experimental results seemed to compare well with the flows predicted by the CFD simulations. The simulations predicted that the improvement in mixing over a straight channel was at best 35%, but typically in the range of 5-10%. Therefore, for this method to be effective, the design would have to be well optimised, performed multiple times through an array of mixers, or coupled with another mixing method.

Table 9 Novel designs summary

Mixing mechanism	Various
CFD models	Various
Validation examples	42, 86
Flow visualisation	Various
Device size	Various
References	42, 86-87

5. ACTIVE MIXING METHODS

In this section, the current practices used to perform active mixing in microfluidic devices shall be discussed. Again, each subsection ends with a table summarising important features and references.

5.1 STIRRER BASED

Stirrers are commonly used in large scale chemical synthesis as an effective means of producing mixing. The device reported in Ref. 88 uses an array of stirrers, actuated by rotating magnetic fields, to produce circulation loops in the flow, producing a significantly mixed flow in the lee of the stirrer. The geometry of the stirrer and mixing channel is shown in Figure 13. Since only the flow in lee of the stirrer is fully mixed, up to the radius of the stirrer from the centreline, it would be necessary to use an array of stirrers, offset so that the flow passing through one stirrer is then mixed with the flow from another.

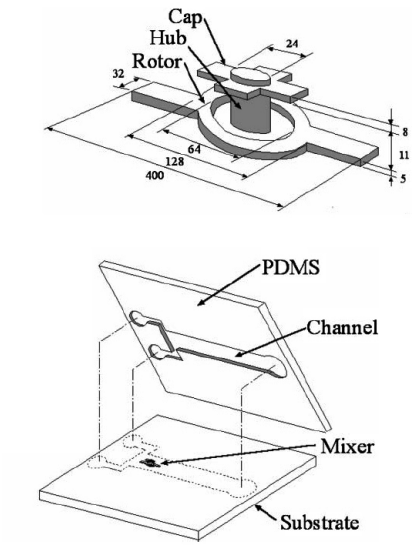

Figure 13 Stir bar geometry (all dims in μm) and mixing channel schematic [source: 88].

This work was continued in Ref. 89, where different mixing geometries were used to mix two fluid streams. Figure 14 shows an optical image of one example studied.

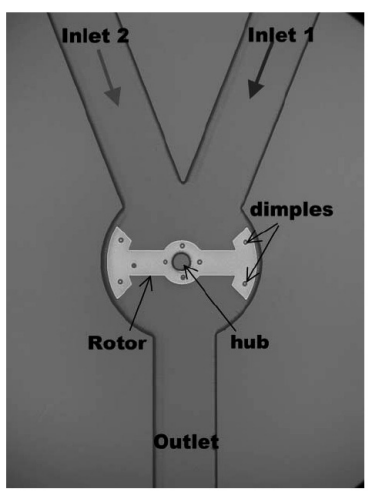

Figure 14 Optical micrograph of a magnetic stir bar, with a rotor diameter of 400 μm [source: 89].

This design produced a significant amount of mixing within 2 seconds of start-up, and as such would only really be useful for continuous flow type processes, or batch processes involving relatively large volumes. The mixing is visualised using food dye, as illustrated in Figure 15.

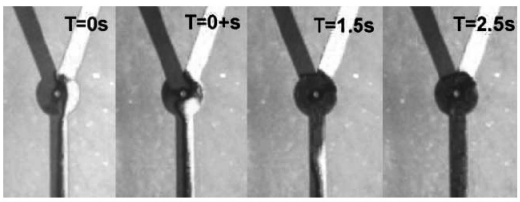

Figure 15 Mixing operation with a stir bar rotation of 150 rpm [source: 89].

Another interesting aspect of this work is that the stir bar can be used as a pump when offset from the main flow channel so that only the part of the bar is in the main flow channel at a time. Flow rates of 60 nL/min were achieved with a rotation of 800 rpm in a 25 μm high, 200 μm wide channel.

CFD modelling of a stir bar has been achieved in Ref. 88, where the stirrer was modelled as sources of momentum, producing rotation in the prescribed area. These simulation results, obtained using CFD-ACE, compared well with the accompanying experimental data.

Table 10 Stirrer summary

Mixing mechanism	Increase in diffusion area Convective fluxes
CFD models	Diffusive scalars Rotational source terms
Validation examples	88
Device size	Typically ∅ 400 μm
References	88-89

5.2 TRANSIENT PULSING & TRANSVERSE MOMENTUM

Another method of inducing mixing is the use of transient pulsing as a method of inducing mixing. With reference to eqn (4), an increase of the transient term will lead to an increase in the diffusive fluxes. Time pulsing has a set of associated dimensionless groups which can be used to characterise the system. The first is the Strouhal number, which represents the ratio of pulsation to inertial forces, and is given as

$$\mathrm{St} = \frac{\omega \cdot d}{u} \tag{16}$$

where ω is the frequency of the pulsations. Another important dimensionless group is the Womersley number, which is the ratio of pulsation to viscous forces, and is given as

$$\mathrm{Wo} = d\sqrt{\frac{\omega}{\upsilon}} \tag{17}$$

where υ is the kinematic viscosity. Generally, the higher the Strouhal and Womersley number, the faster the mixing process.

In the case of transverse momentum pulsing, where the flow is pulsed in a direction

normal to the bulk flow direction, then the pulsing results in a distortion of the concentration profile, increasing the diffusion area.

The work reported in Ref. 27 used pulsing from a single side channel normal to the main channel to induce mixing, with the fluids entering one each from either channel. The work, which was simulation based, examined sinusoidal pulsing of just the side channel, and then both together in different phase alignments, namely 90° and 180° out of phase. Pulsing only the side channel inlet caused a slight increase in the diffusion layer between the two liquids, although the flow remained strongly heterogeneous. The 90° out of phase pulsing significantly increased the mixing, with the diffusion layer extending across the entire main channel. The 180° out of phase pulsing produce a very different affect on the concentration profile, with longitudinal peaks and troughs in concentration, termed 'puffs' by the authors, being the result. These distorted puffs would increase the diffusion area, and as such would increase the mixing rate. The draw back of the method described in Ref. 27 is that only a single side channel was utilised, leading to asymmetries in the flow, and a lack of mixing in the region of the wall opposite the side channel entrance.

Others have reported using similar transverse pumping strategies in their devices (Refs. 28, 90 & 91), with various takes on the same principle.

Table 11 Transverse pumping summary

Mixing mechanism	Increase in diffusion area Convective fluxes
CFD models	Diffusive scalars Transient boundary conditions
Validation examples	27
Device size	Various
References	27-28, 90-91

5.3 ELECTROKINETIC METHODS

Electrokinetic methods encompass magnetohydrodynamics, electroosmosis and electrophoresis. Magnetohydrodynamics examines the use of magnetic fields to influence the behaviour of an electrically conducting fluid. Electroosmotic flow (EOF) is the motion of an ionised liquid relative to a charged surface, whereas electrophoresis is the motion of charged particles suspended within a liquid, although both are induced by the application of an electric field. All three categories have the potential as tools for aiding in the mixing process, and have been reported as such in the literature.

In the paper Ref. 92, dielectrophoresis was used to distort a stream of suspended polystyrene particles by periodic switching of an applied electric field. Dielectrophoresis is the motion of initially neutral particles that are polarised by the presence of a non-uniform electric field (Ref. 93). In this example, the electric fields were used in conjunction with a sudden expansion/contraction section, resulting in chaotic motion, distorting the concentration profile.

The paper Ref. 94 examined the effect of electrophoresis on parameters such as diffusivity and velocity of the particles involved in an enzyme-linked immunoassay, and finally modelled an entire immunoassay cycle.

The device reported in Ref. 95 use magnetohydrodynamics to drive the flow within an annular microchannel. The device is intended for use with a DNA amplification reaction, a

cyclic process particularly suited to continuous rotational flow. The work reported in Ref. 96 uses magnetohydrodynamic methods to produce counter-rotating vorticies, which has a two dimensional stirring effect on the flow, which is translated to the third dimension by Ekman pumping (see Figure 16).

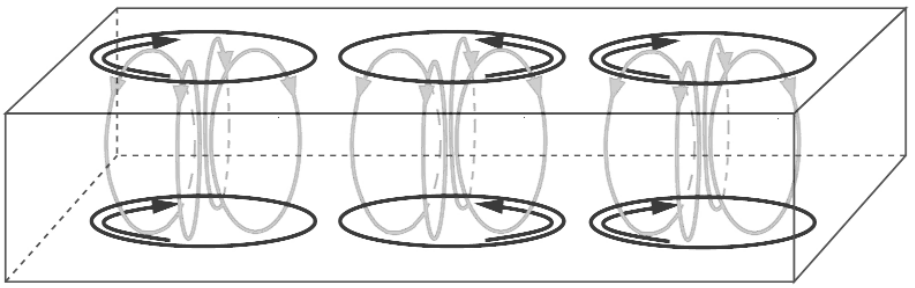

Fig. 16 Schematic of magnetohydrodynamic singularity induced stirring (dark) with Ekman pumping (light) [source: 96].

The device reported in Ref. 97 used a simple multi-lamination based micromixer to combine two streams into 15 striations, the difference being that an electroosmotic pump was used to drive the flow.

Table 12 Electrokinetic summary

Mixing mechanism	Increase in diffusion area Convective fluxes
CFD models	Diffusive scalars Electrokinetics Transient boundary conditions
Validation examples	98, 99
Device size	Various
References	92-100

5.4 ACOUSTIC & ULTRASONIC MIXERS

Acoustic methods induce vibrations in the flow, with fluid naturally migrating towards the nodes of vibration. The devices reported in Ref. 101 used static and rotating arrays of vibrating transducers to induce bulk motion in the fluid. The arrangements of the transducers was such that rotational flows were induced, producing mixing.

The device reported in Refs. 102 & 103 uses acoustics to vibrate a bubble or multiple bubbles within the mixing chamber, leading to homogenisation within two minutes.

Ultrasonic devices, a sub-section of acoustic devices, work on two principles, three if the use of ultrasound to provide the flow with a driving force is included, and then some other method to actually achieve the mixing. One mixing method is simple vibration, which increases both the transient and convective terms of eqn (2). Another is the inducement of chaotic advection, which increases the convection terms of eqn (2), and causes distortion of the concentration profile, increasing the diffusion area.

The work reported in Ref. 104 uses ultrasound to exert a body force on the fluid, driving the fluid through the device. The acoustic signal is attenuated by the fluid, which absorbs the energy, converting it into kinetic energy. The mixer design described briefly in this work uses alternate pulsing of the fluid to induce mixing.

The work described in Refs. 105 & 106 uses ultrasonic vibration to induce mixing by way of a diaphragm. Small scale turbulent or chaotic advection flow patterns are observed, mixing the fluids within the relatively long time of two seconds. These papers are especially useful since significant space is dedicated to highlighting the problems with the current designs, and to the method in general. Temperature rises associated with ultrasonic excitation are discussed, along with the possibility of combining ultrasonic mixing with some of the static structures described earlier.

Table 13 Acoustic & ultrasonic summary

Mixing mechanism	Increase in diffusion area Convective fluxes
CFD models	Diffusive scalars Transient boundary conditions
Validation examples	101
Device size	Typically 16 x 16 x 0.2 mm
References	101-106

6. DISCUSSION

There are a number of different methods for achieving mixing in micro-channels reported in the available literature. The common method of classification is to split designs into passive or active mixing methods; passive if the fluid naturally mixes, either by local geometry, or due to the presence of free surfaces, or active if external energy and moving parts are required. Devices can be classified in other ways, depending on their suitability for certain applications. Certain mixers, such as turbulent junction or jet mixers, only really lend themselves to continuous flow processes due to the high flow rates required to achieve transitional turbulent flow. On the other hand, droplet based mixers are best suited to batch processes (Ref. 12), since bubble injection and then subsequent removal could prove problematic. Aside from the question of continuous or batch process suitability, the actual application is important, i.e. what will the mixer be mixing. Chemical synthesis and biological/chemical reactions systems more commonly use micro mixers at the heart of their devices, and can be very sensitive to temperature rises, or in cases where long chain polymers are held in suspension, regions of high shear can damage the molecules.

In terms of the fluid behaviour visible in these devices, there are some points of real interest. The majority of the reported devices manipulate flows that are laminar in nature. Some devices however, such as the junction and jet based methods, utilise the onset of turbulence to increase mixing. In laminar devices, which are diffusion limited, lower flow rates are preferable since the increased residence time gives greater time for diffusion to occur. In turbulent devices however, the higher the flow rate the more turbulent the flow, and therefore the better the mixing.

One source of confusion that should be clarified is the difference between turbulence and chaotic advection, as used in the literature surrounding this subject area. Advection can be defined as the transport of something (such as a species, particles, concentration etc) from

one region to another. Therefore advection relates much more directly to mixing than turbulence does, since turbulence can be present in pure fluids, whereas advection relates specifically to some particular substance moving relative to another. Chaotic motion can be defined as apparently being disordered or highly sensitive to perturbation, although randomness is never associated with chaos, since chaos allows for cause and effect. Turbulence is often classified as a chaotic motion, since it has recognisable structures such as eddies, and as such, even though instantaneous values are difficult to predict, bulk time-averaged behaviour can be quantified. To correctly differentiate between turbulence and chaotic advection when referring to micro mixing events, it is necessary to examine the sources of the two phenomena. When quantifying turbulence, the Reynolds number is often the most important parameter. As previously mentioned, the Reynolds number is the ratio of inertial to viscous forces, and when viscosity is significant in comparison to inertia, then unsteady fluctuations are damped out by viscous action. However, when inertia dominates over viscosity, unsteady recirculation eddy motions become apparent, giving rise to turbulence. It can therefore be said that turbulence is the result of the fluid having very large inertia compared to its viscosity, and that any minor perturbations will result in turbulence. With chaotic advection, even though the inertia is still larger than the viscosity, it does not dominate, and chaotic advection is the result of streamlines and currents brought about by geometrical features, not due to the insignificance of viscosity. Another feature of turbulent flow is the continuous cascade of motion length scales down to the smallest or Kolmogorov length scale (Ref. 21). This feature of the flow is not necessarily present in chaotic advection.

Active methods tend to have moving parts, and as such may have reliability issues, but can offer superior mixing to passive methods. Stirrer based methods offer complete mixing within very small geometries, but do so with relatively high angular velocities, and suffer from blockage problems if particulates are involved. Magnetohydrodynamic stirrers avoid this problem by not having any moving parts in contact with the flow, although similar mixing speeds are difficult to achieve. Driving force pulsing methods offer excellent and efficient mixing, although again they rely on the motion of values and actuators for their operation. Acoustic and ultrasonic mixers perform well enough, although kinetic heating, rapid vibrations and reliability are all issues for industrial use.

Optimisation methods have been applied to only a few of the systems reviewed (Refs. 28, 58 & 69). This could help to ensure that mixing systems perform efficiently, and as such a complete understanding of the flow is required. Problems such as stagnation zones, kinetic heating and flow reversibility often need to be avoided to ensure efficient operation. Parameters such as residence time and diffusion area need to be maximised for laminar flow types, whereas high flow rates are required for turbulent mixers.

Much of the work that has been reported concerns liquid/liquid or gas/gas mixing, with some work on liquid/gas mixing. Some areas that are not widely reported are the mixing of gases and liquids with solid macro particles. Many chemical and biological assays are performed with solid label particles, and little has been reported concerning inter-particle interactions and the geometries and fabrication methods suitable to suspended particle transport.

With regard to the level of coupling between the flow dynamics and the mixing process, much of the work reported thus far can be characterised as level 1, since the products of the mixing process do not significantly influence the flow field. Dye visualisation methods are a widespread method of mixing quantification, but are only characteristic of level 1 systems. For example, if a mixer relies on turbulent action, if the product of the process has significantly lower density or higher viscosity then the turbulent action may be dissipated,

reducing any subsequent mixing downstream. Or, in the case of surface tension driven flows, chemical reaction products may act to reduce surface tension, affecting the driving force.

A few studies have been reported concerning highly exothermic reactions in micro mixers (Ref. 107 & 108), and the effect of this heat source on the overall flowfield, and therefore the mixing efficiency. Since micro-propulsion and micro gas turbines are becoming a more popular research topic, channel geometries and flow rates will have to be optimised for efficient fuel usage. The problems of experimental validation are highlighted in Ref. 108, where temperature gradients along thermocouples led to slightly inaccurate readings.

In terms of effectiveness and efficiency, methods based around multi-laminate methods appear to out perform devices of other types. The massive increase in diffusion area means that diffusion occurs at rates that vary directly with the number of laminae. Split/recombination methods, being a type of multi-lamination are also very effective, although many multi-laminate devices split the flow into multiple streams in one step, and therefore create more laminae per step than the traditional SAR mixer. Devices that utilise the onset of turbulence get around the problem of diffusion limited mixing altogether, although the high fluid shear involved may not suit all applications. Chevron surface structures definitely induce significant mixing, and are probably suitable to higher flow rates than multi-laminate methods since little constriction of the channel is required. Channel tortuosity has been proved to be very effective at mixing, and so long as stagnation zones can be avoided, could provide an effective solution to both continuous and batch processing. Droplet based mixers have received much less attention than the other methods, most likely in part to the batch method in which individual droplets must be handled. However, the internal rolling motion of droplets has proved to be a very efficient mixing mechanism, and probably deserves greater attention, especially when small volumes are involved.

Computational Fluid Dynamics (CFD) has been a valuable tool for researchers in this field, many of which have reported good agreement between simulation and experimental results. The validation work reported in Ref. 49 described efforts to model the flowfield in a simple T-junction mixer. Simulation results predicted the three flow regimes common to these microdevices (laminar, vortex and engulfment), and further experimental investigation confirm the correctness of the results. The work reported in Ref. 67 used particle tracking to examine the flow in a chevron patterned chaotic advection micromixer. In this work the mass and velocity fields are solved as a steady state problem, and then the flowfield variables are stored and used as the basis for a transient particle tracking simulation. The results are in qualitative agreement with mixers of this type (see Figures 8 and 9), although work is still progressing to fully validate this method. The work reported in Ref. 101 concerning acoustic bubble mixing used a harmonic wall velocity boundary condition to mimic the effect of a vibrating bubble. This technique captured the main features of the flow, and agreed with experiment in so far as predicting the layouts that were favourable and unfavourable for mixing.

The physics and techniques involved in the applications described above are all well within the capability of most commercial CFD solvers. However the influence of electric fields is still not offered by all solvers, and adds an extra level of coupling within the solution which can prove problematic for certain applications. The work described in Ref. 99 used CFD-ACE to model an electroosmotic flow problem, and predicted mixing lengths that agreed very well with the accompanying experiment. A chevron pattern of electrodes was used to induce a lateral oscillation as the flow passed over them, leading to rapid mixing. Again, CFD-ACE was used in Ref. 100 to model an electroosmotic flow problem, with experimental results providing excellent validation of the numerical model. It has therefore been demonstrated that effective multiphysics flow solvers are commercially available.

Overall, there are a number of established methods of mixing in microscale geometries, such as multi-lamination and surface structures. There also seems to be a continuous supply of novel mixing methods, although all employ variations on the basic rules of increasing diffusion area, residence time and convection. Turbulent mixing is achievable for continuous flow configurations, and is suitable so long as high strain regions are not an issue, as they are for suspended polymers and biological components. Combining methods such as multi-lamination and flow focusing have produced promising results, and could be extended to incorporate chaotic advection and pulsing methods. A significant amount of material has been published with regard to transverse pumping methods, although little has been reported regarding in-line pumping, and as such remains a topic of interest. Droplet methods appear to offer excellent mixing in microlitre and smaller sample sizes, and as such have application in biological assay devices such as blood or urine tests. Flow splitting methods have been developed to such an extent that large samples can be broken down into smaller droplets allowing multiple assays to be conducted within a single device, thus rivalling more traditional lab based methods within the medical industry.

7. CONCLUDING REMARKS

Mixing in microscale geometries is challenging since flows are generally laminar, and consequently the mixing is diffusion-limited. The area of micro mixing is still developing, although many of the earliest methods are now well documented. Both established and more novel methods have been reviewed here, and their relative strengths and weakness for various applications discussed. Passive mixers use channel geometries and natural fluid behaviour to induce mixing, whereas active mixers use an external power source, and often involve either moving parts or electrodes. Active mixers are capable of producing more rapid mixing than passive methods, although this is often offset a reduction in reliability and the requirement to provide a power source.

In order to optimise devices, parameters such as flow rate (residence time), diffusion area and geometry need to be considered. CFD has proved to be a useful tool in the design and analysis of micro-mixing devices, and has been well validated for such diverse methods as acoustic mixing, T-junction mixers and electro-kinetic methods. Most researchers in this field report either experimental results or a combination of numerical simulation and experimental validation, and often describe the fabrication process, since this too is a developing field. Very rarely do researchers published simulation results without attempting to validate it against either their own work or that of others. Newer flow solvers that are more inclined towards multiphysics modelling are generally used, since the more established solvers typically do not perform as well when modelling such effects as surface tension and electrokinetic behaviour. The most popular experimental flow visualisation method is dye, although seeded particles coupled with various interrogation methods are gaining popularity. Image processing is used to quantify the mixing from experimental data, whereas subroutines based around the calculation of standard deviation are the most popular method of quantifying mixing from results produced by numerical simulation.

REFERENCES

1. deMello, A. & Wootton R., But what is it good for? Applications of microreactor technology for the fine chemical industry, *Lab on a Chip*, 2002, 2, 7N-13N.
2. Hessel, V. & Löwe, H., Microchemical Engineering: Components, Plant Concepts User Acceptance - Part I, *Chem. Eng. Technol*., 2003a, 26, 13-24.
3. Hessel, V. & Löwe, H., Microchemical Engineering: Components, Plant Concepts User Acceptance - Part II, *Chem. Eng. Technol*., 2003b, 26, 391-408.

4. Hessel, V. & Löwe, H., Microchemical Engineering: Components, Plant Concepts User Acceptance - Part III, *Chem. Eng. Technol*., 2003c, 26, 531-544.
5. Kestenbaum, H., de Oliveira, A.L., Schmidt, W., Schüth, F., Ehrfeld, W., Gebauer, K., Löwe, H., Richter, T., Lebiedz, D., Untiedt, I. & Züchner, H., Silver-Catalyzed Oxidation of Ethylene to Ethylene Oxide in a Microreaction System, *Ind. Eng. Chem.* Res., 2002, 41, 710-719.
6. Shah, K., Ouyang, X. & Besser, R.S., Microreaction for Microfuel Processing: Challenges and Prospects, *Chem. Eng. Technol*., 2005, 28, 303-313.
7. Kamholz, A.E., Weigl, B.H., Finlayson, B.A. & Yager, P., Quantitative Analysis of Molecular Interaction in a Microfluidic Channel: The T-Sensor, *Anal. Chem*., 1999, 71, 5340-5347.
8. Kamholz, A.E., Schilling, E.A. & Yager, P., Optical Measurement of Transverse Molecular Diffusion in a Microchannel, *Biophys. J*., 2001, 80, 1967-1972.
9. Burns, M.A., Johnson, B.N., Brahmasandra, S.N., Hanique, K., Webster, J.R., Krishnan, M., Sammarco, T.S., Man, P.M., Jones, D., Heldsinger, D., Mastrangelo, C.H. & Burke, D.T., An Integrated Nanoliter DNA Analysis Device, *Science*, 1998, 282, 484-487.
10. Hayes, M.A., Polson, N.A., Phayre, A.N. & Garcia, A.A., Flow-Based Microimmunoassay, *Anal. Chem*., 2001, 73, 5896-5902.
11. Ko, J.S., Yoon, H.C., Yang, H., Pyo, H.B., Chung, K.H., Kim, S.J. & Kim, Y.T., A polymer-based microfluidic device for immunosensing biochips, *Lab on a Chip*, 2003, 3, 106-113.
12. Srinivasan, V., Pamula, V.K. & Fair, R.B. An integrated digital microfluidic lab-on-a-chip for clinical diagnostics on human physiological fluids, *Lab on a Chip*, 2004, 4, 310-315.
13. Jensen, K.F., Microreaction engineering - is small better?, *Chem. Eng. Sci*., 2001, 56, 293-303.
14. McBride, M.T., Gammon, S., Pitesky, M., O'Brien, T.W., Smith, T., Aldrich, J., Langlois, R.G., Colston, B. & Venkateswaran, K.S., Multiplexed Liquid Arrays for Simultaneous Detection of Simulants of Biological Warfare Agents, *Anal. Chem*., 2003, 75, 1924-1930.
15. Neuman, M.R., Fair, R.B., Mehregany M. & Massoud, H.Z., Microelectromechanical Systems: A New Technology for Biomedical Applications, *IEEE*, 1993, 1545-1546.
16. Oki, A., Ogawa, H., Nagai, M., Shinbashi, S., Takai, M., Yokogawa A. & Horiike, Y., Development of healtcare chips checking life-style-related diseases, *Mat. Sci. Eng*. C, 2004, 24, 837-843.
17. Reyes, D.R., Iossifidis, D., Auroux, P.A. & Manz, A., Micro Total Analysis Systems. 1. Introduction, Theory, and Technology, *Anal. Chem*., 2002, 74, 2623-2636.
18. Auroux, P.A., Iossifidis, D., Reyes, D.R. & Manz, A., Micro Total Analysis Systems. 2. Analytical Standard Operations & Applications, *Anal. Chem*., 2002, 74, 2637-2652.
19. Jensen, K., Smaller, faster chemistry, *Nature*, 1998, 393, 735-737.
20. Houghton, P., *Microfluidics Mixing Laboratory*, MEMS Course Notes, University of Hertfordshire, 2004.
21. Dimotakis, P.E., Turbulent Mixing, *Annu. Rev. Fluid Mech*., 2005, 37, 329-56.
22. Patankar, S.V., *Numerical Heat Transfer and Fluid Flow*, Hemisphere Publishing Corp., New York, 1980, 12-13.
23. Probstein, R.F., *Physicochemical Hydrodynamics - An Introduction*, 2nd edn., Wiley Interscience, New York, 1994, 116-123.
24. Chapman, B.K. & Leighton, D.T., Dynamic Viscous Resuspension, *Int. J. Multiphase Flow*, 1991, 17, 469-483.
25. Leighton, D. & Acrivos, A., Viscous Resuspension, *Chem. Eng. Sci*., 1986, 41, 1377-1384.
26. Philips, R.J., Armstrong, R.C., & Brown, R.A., A consitutive equation for concentrated suspensions that account for shear-induced particle migration, *Phys. Fluids A*, 1992, 4, 30-40.
27. Glasgow, I. & Aubry, N., Enhancement of microfluidic mixing using time pulsing, *Lab on a Chip*, 2003, 3, 114-120.
28. Müller, S.D., Mezić, I., Walther, J.H. & Koumoutsakos, P., Transverse momentum micromixer optimization with evolution strategies, *Computers & Fluids*, 2004, 33, 521-531.

29. Tsai, J. & Lin, L., Active microfluidic mixer and gas bubble filter driven by thermal bubble micropump, *Sens. Actu. A*, 2002, 0, 665-671.

30. Baier, T., Drese, K.S., Schönfeld, F. & Schwab, U., A μ-Fluidic Mixing Network, *Chem. Eng. Technol.*, 2005, 28, 362-366.

31. Beebe, D.J., Adrian, R.J., Olsen, M.G., Stremler, M.A., Aref H. & Jo, B., Passive mixing in microchannels: Fabrication and flow experiments, *Mec. Ind.*, 2001, 2, 343-348.

32. Mengeaud, V., Josserand, J. & Girault, H.H., Mixing Processes in a Zigzag Microchannel: Finite Element Simulations and Optical Study, *Anal. Chem.*, 2002, 74, 4279-4286.

33. Stroock, A.D., Dertinger, S.K.W., Ajdari, A., Mezić, I., Stone H.A. & Whitesides, G.M., Chaotic Mixer for Microchannels, *Science*, 2002, 295, 647-651.

34. Kim, D.J., Oh, H.J., Park, T.H., Choo, J.B. & Lee, S.H., An easily integrative and efficient micromixer and its application to the spectroscopic detection of glucose-catalyst reactions, *Analyst*, 2005, 130, 293-298.

35. Yamaguchi, Y., Takagi, F., Watari, T., Yamashita, K., Nakamra, H., Shimizu, H. & Maeda, H., Interface configuration of the two layered laminar flow in a curved microchannel, *Chem. Eng. J.*, 2004, 101, 367-372.

36. Sandeep, P. & Bisht, P.B., Concentration sensing based on radiative rate enhancement from a single microcavity, *Chem. Phys. Lett.*, 2005, 415, 15-19.

37. Ullman, E.F., Kirakossian, H., Switchenko, A.C., Ishkanian, J., Ericson, M., Wartchow, C.A., Pirio, M., Pease, J., Irvin, B.R., Singh, S., Singh, R., Patel, R., Dafforn, A., Davalian, D., Skold, C., Kurn, N. & Wagner, D.B., Luminescent oxygen channelling assay (LOCITM): sensitive, broadly applicable homogeneous immunoassay method, *Clin. Chem.*, 1996, 42, 1518-1526.

38. Patel, R., Pollner, R., de Keczer, S., Pease, J., Pirio, M., DeChene, N., Dafforn, A. & Rose, S., Quantification of DNA Using the Luminescent Oxygen Channelling Assay, *Clin. Chem.*, 2000, 46, 1471-1477.

39. Koch, M., Witt, H., Evans A.G.R. & Brunnschweiler, A., Improved characterization technique for micromixers, *J. Micromech. Microeng.*, 1999, 9, 156-158.

40. Bökenkamp, D., Desai, A., Yang, X., Tai, Y.C., Marzluff, E.M. & Mayo, S.L., Microfabricated Silicon Mixers for Submillisecond Quench-Flow Analysis, *Anal. Chem.*, 1998, 70, 232-236.

41. Liu, Y.Z., Kim, B.J. & Sung, H.J., Two-fluid mixing in a microchannel, *Int. J. Heat & Fluid Flow*, 2004, 25, 986-995.

42. Chung, Y., Hsu, Y., Jen, C., Lu, M. & Lin, Y., Design of passive mixers utilizing microfluidic self-circulation in the mixing chamber, *Lab on a Chip*, 2004, 4, 70-77.

43. Ottino, J.M., Ranz, W.E. & Macosko, C.W., A lamellar model for analysis of liquid-liquid mixing, *Chem. Eng. Sci.*, 1979, 34, 877-890.

44. Ottino, J.M., Lamellar mixing models for structured chemical reactions and their relationship to statistical models; macro and micromixing and the problem of averages, *Chem. Eng. Sci.*, 1980, 35, 1377-1391.

45. Bessoth, F.G., deMello, A.J., & Manz, A., Microstructure for efficient continuous flow mixing, *Anal. Commun.*, 1999, 36, 213-215.

46. Koch, M., Schabmueller, C.G.J., Evans, A.G.R. & Brunnschweiler, A., Micromachined chemical reaction system, *Sens. Actu. A*, 1999, 74, 207-210.

47. Freitas, S., Walz, A., Merkle, H.P. & Gander, B., Solvent extraction employing a static micromixer: a simple, robust and versatile technology for the microencapsulation of proteins, *J. Microencapsulation*, 2003, 20, 67-85.

48. Löb, P., Pennemann, H. & Hessel, V., g/l-Dispersion in interdigital micromixers with different mixing chamber geometries, *Chem. Eng. J.*, 2004, 101, 75-85.

49. Engler, M., Kockmann, N., Kiefer, T. & Woias, P., Numerical and experimental investigations on liquid mixing in static micromixers, *Chem. Eng. J.*, 2004, 101, 315-322.

50. Haeberle, S., Brenner, T., Schlosser, H.P., Zengerle, R. & Ducrée, J., Centrifugal Micromixer, *Chem. Eng. Technol.*, 2005, 28, 613-616.

51. Holden, M.A., Kumar, S., Beskok, A. & Cremer, P.S., Microfluidic diffusion diluter: bulging of PDMS microchannels under pressure-driven flow, *J. Micromech. Microeng.*, 2003, 13, 412-418.

52. Blood, P.J., Denyer, J.P., Azzopardi, B.J., Poliakoff, M. & Lester, E., A versatile flow visualisation technique for quantifying mixing in a binary system: application to continuous supercritical water hydrothermal synthesis (SWHS), *Chem. Eng. Sci*, 2004, 59, 2853-2861.

53. Wong, S.H., Bryant, P., Ward, M. & Wharton, C., Micro T-mixer as a rapid mixing micromixer, *Sens. Actu. B*, 2004, 100, 359-379.

54. Gobby, D., Angeli, P. & Gavriilidis, A., Mixing characteristics of T-type microfluidic mixers, *J. Micromech. Microeng*., 2001, 11, 126-132.

55. Johnson, T.J., Ross, D. & Locascio, L.E., Radpid Microfluidic Mixing, *Anal. Chem*., 2002, 74, 45-51.

56. Wong, S.H., Bryant, P., Ward, M. & Wharton, C., Investigation of mixing in a cross-shaped micromixer with static mixing elements for reaction kinetics studies, *Sens. Actu. B*, 2003, 95, 414-424.

57. Branebjerg, J., Gravesen, P., Krog J.P. & Nielsen, C.R., Fast mixing by lamination, *IEEE*, 1996, 441-446.

58. Schönfeld, F., Hessel, V. & Hoffmann, C., An optimised split-and-recombine micro-mixer with uniform 'chaotic' mixing, *Lab on a Chip*, 2004, 4, 65-69.

59. Bertsch, A., Heimgartner, S., Cousseau, P. & Renaud, P., 3D Micromixers - Downscaling Large Scale Industrial Static Mixers, *IEEE*, 2001, 507-510.

60. Kim, D.S., Lee, S.H., Kwon, T.H. & Ahn, C.H., A serpentine laminating micromixer combining slitting/recombination and advection, *Lab on a Chip*, 2005, 5, 739-747.

61. Neils, C., Tyree, Z., Finlayson, B. & Folch, A., Combinatorial mixing of microfluidic streams, *Lab on a Chip*, 2004, 4, 342-350.

62. Jiang, F., Drese, K.S., Hardt, S., Küpper, M. & Schönfeld, F., Helical flows and Chaotic Mixing in Curved Micro Channels, *AIChE Journal*, 2004, 50, 2297-2305.

63. Xia, H.M., Wan, S.Y.M., Shu, C. & Chew, Y.T., Chaotic micromixers using two-layer crossing channels to exhibit fast mixing at low Reynolds numbers, *Lab on a Chip*, 2005, 5, 748-755.

64. Stroock, A.D., Dertinger, S.K., Whitesides, G.M. & Ajdari, A., Patterning Flows Using Grooved Surfaces, *Anal. Chem*., 2002, 74, 5306-312.

65. Kang, T.G. & Kwon, T.H., Colored particle tracking method for mixing analysis of chaotic micromixers, *J. Micromech. Microeng*., 2004, 14, 891-899.

66. Howell, P.B., Mott, D.R., Fertig, S., Kaplan, C.R., Golden, J.P., Oran, E.S. & Ligler, F.S., A microfluidic mixer with grooves placed on the top and bottom of the channel, *Lab on a Chip*, 2005, 5, 524-530.

67. Aubin, J., Fletcher, D.F. & Xuereb, C., Design of micromixers using CFD modelling, *Chem. Eng. Sci*., 2005, 60, 2503-2516.

68. Veenstra, T.T., Lammerink, T.S.J., Elwenspoek, M.C., & van den Berg, A., Characterization method for a new diffusion mixer applicable in micro flow injection analysis systems, *J. Micromech. Microeng*., 1999, 9, 199-202.

69. Drese, K.S., Optimization of interdigital micromixers via analytical modeling - exemplified with SuperFocus mixer, *Chem. Eng. J*., 2004, 101, 403-407.

70. Dussan,V E.B. & Davis, S.H., On the motion of a fluid-fluid interface along a solid surface, *J. Fluid Mech*, 1974, 65, 71-95.

71. Huh, C. & Scriven, L.E., Hydrodynamic model of steady movement of a solid/liquid/fluid contact line, *J. Coll. Int. Sci*, 1971, 37, 196-207.

72. Duda, J.L. & Vrentas, J.S., Steady Flow in the Region of Closed Streamlines II Cylindrical Cavity, *J. Fluid Mech*, 1971, 45, 247-260.

73. Fowler, J., Moon, H. & Kim, C., Enhancement of Mixing by Droplet-Based Microfluidics, *IEEE*, 2002, 97-100.

74. Hosokawa, K., Fujii, T. & Endo, I., Handling of Picoliter Liquid Samples in a Poly(dimethylsiloxane)_Based Microfluidic Device, *Anal. Chem*., 1999, 71, 4781-4785.

75. Prins, M.W.J., Welters, W.J.J. & Weekamp, J.W., Fluid Control in Multichannel Structures by Electrocapillary Pressure, *Science*, 2001, 291, 277-280.

76. Pollack, M.G., Shenderov, A.D. & Fair, R.B., Electrowetting-based actuation of droplets for integrated microfluidics, *Lab on a Chip*, 2002, 2, 96-101.

77. Zeng, J. & Korsmeyer, T., Principles of droplet electrohydrodynamics for lab-on-a-chip, *Lab on a Chip*, 2004, 4, 265-277.

78. Paik, P., Pamula, V.K., Pollack, M.G. & Fair, R.B., Electrowetting-based droplet mixers for microfluidic systems, *Lab on a Chip*, 2003a, 3, 28-33.

79. Paik, P., Pamula, V.K. & Fair, R.B., Rapid droplet mixers for digital microfluidic systems, *Lab on a Chip*, 2003b, 3, 253-259.

80. Handique, K. & Burns, M.A., Mathematical modeling of drop mixing in a slit-type microchannel, *J. Micromech. Microeng.*, 2001, 11, 548-554.

81. Ariyapadi, S., McMillan, J., Zhou, D., Berruti, F., Briens, C. & Chan, E., Modeling the mixing of a gas-liquid spray jet injected in a gas-solid fluidized bed: The effect of the draft tube, *Chem. Eng. Sci.*, 2005, 60, 5738-5750.

82. Kouakou, E., Salmon, T., Toye, D., Marchot, P. & Crine, M., Gas-liquid mass transfer in a circulating jet-loop nitrifying MBR, *Chem. Eng. Sci.*, 2005, 60, 6346-6353.

83. Miyake, R., Lammerink, T.S.J., Elwenspoek, M. & Fluitman, J.H.J., Micro Mixer with Fast Diffusion, *IEEE*, 1993, 248-253.

84. Ehlers, St., Elgeti, K., Menzel, T. & Wießmeier, G., Mixing in the offstream of a microchannel system, *Chem. Eng. Processing*, 2000, 39, 291-298.

85. Cherepanov, A.V., & de Vries, S., Microsecond freeze-hyperquenching: development of a new ultrafast micro-mixing and sampling technology and application to enzyme catalysis, *Biochimica & Biophysica*, 2004, 1656, 1-31.

86. Hong, C., Choi, J. & Ahn, C.H., A novel in-plane passive microfluidic mixer with modified Tesla structures, *Lab on a Chip*, 2004, 4, 109-113.

87. Kuksenok, O., Yeomans, J.M. & Balazs, A.C., Using patterned substrates to promote mixing in microchannels, *Phys. Rev. E.*, 2002, 65, 031502.

88. Lu, L.H., Ryu, K.S. & Liu, C., A Magnetic Microstirrer and Array for Microfluidic Mixing, *J. MEMS*, 2002, 11, 462-469.

89. Ryu, K.S., Shaikh, K., Goluch, E., Fan, Z. & Liu, C., Micro magnetic stir-bar mixer integrated with parylene microfluidic systems, *Lab on a Chip*, 2004, 4, 608-613.

90. Niu, X. & Lee, Y.K., Efficient spatial-temporal chaotic mixing in microchannels, *J. Micromech. Microeng.*, 2003, 13, 454-462.

91. Dodge, A., Jullien, M., Lee, Y., Niu, X., Okkels, F. & Tabeling, P., An example of a chaotic micromixer: the cross-channel micromixer, *C. R. Physique*, 2004, 5, 557-563.

92. Lee, Y., Deval, J., Tabeling, P. & Ho, C., Chaotic Mixing in Electrokinetically and Pressure Driven Micro Flows, *Proc. 14th IEEE MEMS*, 2001, , 483-486.

93. Karniadakis, G.E. & Beskok, A., *Micro Flows - Fundamentals and Simulation*, Springer-Verlag, New York, 2002, 215-221.

94. Přibyl, M., Šnita, D., Hasal, P. & Marek, M., Modeling of electric-field driven transport processes in microdevices for immunoassay, *Chem. Eng. J.*, 2004, 101, 303-314.

95. West, J., Karamata, B., Lillis, B., Gleeson, J.P., Alderman, J., Collins, J.K., Lane, W., Mathewson, A. & Berney, H., Application of magnetohydrodynamic actuation to continuous flow chemistry, *Lab on a Chip*, 2002, 2, 224-230.

96. Solomon, T.H. & Mezi_, I., Uniform resonant chaotic mixing in fluid flows, *Nature*, 2003, 425, 376-380.

97. Guenat, O.T., Ghiglione, D., Morf, W.E. & de Rooij, N.F., Partial electroosmotic pumping in complex capillary systems - Part 2: Fabrication and application of a micro total analysis system (_TAS) suited for continuous volumetric nanotitrations, *Sens. Actu.* B, 2001, 72, 273-282.

98. Fu, L.M., Yang, R.J. & Lee, G.B., Electrokinetic Focusing Injection Methods on Microfluidic Devices, *Anal. Chem.*, 2003, 75, 1905-1910.

99. Wu, H. & Liu, C., A novel electrokinetic micromixer, *Sens. Actu.* A, 2005, 118, 107-115.

100. Lin, J.L., Lee, K.H. & Lee, G.B., Active micro-mixers utilizing a gradient zeta potential induced by inclined buried shielding electrodes, *J. Micromech. Microeng.*, 2006, 16, 757-768.

101. Vivek, V., Zeng, Y. & Kim, E.S., Novel Acoustic-Wave Micromixer, *Proc. IEEE*, 2000, 668-673.

102. Liu, R.H., Yang, J., Pindera, M.Z., Athavale, M. & Grodzinski, P., Bubble-induced acoustic micromixing, *Lab on a Chip*, 2002, 2, 151-157.

103. Liu, R.H., Lenigk, R., Druyor-Sanchez, R.L., Yang, J. & Grodzinski, P., Hybridization Enhancement Using Cavitation Microstreaming, *Anal. Chem.*, 2003, 75, 1911-1917.

104. Rife, J.C., Bell, M.I., Horwitz, J.S., Kabler, M.N., Auyeung, R.C.Y. & Kim, W.J., Miniature valveless ultrasonic pumps and mixers, *Sens. Actu. A*, 2000, 86, 135-140.

105. Yang, Z., Goto, H., Matsumoto, M. & Maeda, R., Ultrasonic micromixer for microfluidic systems, *IEEE*, 2000, 80-85.

106. Yang, Z., Matsumoto, S., Goto, H., Matsumoto, M. & Maeda, R., Ultrasonic micromixer for microfluidic systems, *Sens. Actu. A*, 2001, 93, 266-272.

107. Schneider, M.A., Maeder, T., Ryser, P. & Stoessel, F., A microreactor-based system for the study of fast exothermic reactions in liquid phase: characterisation of the system, *Chem. Eng. J.*, 2004, 101, 241-250.

108. Shan, X.C., Wang, Z.F., Jin, Y.F., Wu, M., Hua, J., Wong, C.K. & Maeda, R., Studies on a micro combustor for gas turbine engines, *J. Micromech. Microeng.*, 2005, 15, 215-221.